Available online at www.sciencedirect.com
SCIENCE DIRECT®
PERGAMON
International Journal of Heat and Mass Transfer 46 (2003) 3593–3603
International Journal of HEAT and MASS TRANSFER
www.elsevier.com/locate/ijhmt

Multi-group full-spectrum k-distribution database for water vapor mixtures in radiative transfer calculations

Hongmei Zhang [1], Michael F. Modest *

Department of Mechanical and Nuclear Engineering, The Pennsylvania State University, 301C Reber Building, University Park, PA 16802, USA

Received 21 November 2002; received in revised form 15 March 2003

Abstract

A thorough investigation of the absorption coefficient dependence on temperature and pressure has been performed for water vapor and a 32-group database has been assembled for H_2O mixtures at atmospheric pressure, based on the multi-group full-spectrum correlated k-distribution model. The method is fully scalable, i.e., spectral groups from the database can be combined to obtain coarser group models ($N = 1, 2, 4, \ldots$) for greater numerical efficiency (accompanied by slight loss in accuracy). The databases for CO_2 and H_2O, together with the random-overlap mixture model have been used to simulate a practical combustion problem.

1. Introduction

Radiative transfer in absorbing–emitting gas mixtures can be most accurately predicted using the line-by-line approach, but LBL calculations require large computer resources and computational time. It has been known for some time that, for a narrow spectral range (i.e., a range over which the Planck function $I_{b\eta} \simeq$ const) in a homogeneous medium (i.e., absorption coefficient κ_η is not a function of spatial location), the absorption coefficient may be reordered into a monotonic k-distribution, which produces exact results at a tiny fraction of the computational cost [1,2]. As with other narrow band models, treatment of nonhomogeneous media is somewhat problematic. Two methods have been commonly used to address nonhomogeneity: the scaling approximation and the assumption of a correlated k-distribution. The correlated-k method has been shown to be accurate primarily for low temperature meteorological applications [1,3,4].

More recently, the reordering concept has also been applied to the full spectrum. Denison and Webb [5,6] developed the spectral-line-based weighted-sum-of-gray-gases (SLW) model, in which line-by-line databases are used to calculate weight factors for the popular weighted-sum-of-gray-gases (WSGG) model [7,8]; for nonhomogeneous gases they used the correlated-k approach. A similar method, called the absorption distribution function (ADF) approach, was developed by Rivière et al. [9,10]. Modest and Zhang [11–13] obtained k-distributions for the entire spectrum, showing that the SLW/ADF/WSGG methods are simply crude step implementations of the full-spectrum k-distribution (FSK) method. For nonhomogeneous media the FSK method then becomes the full-spectrum correlated k-distribution (FSCK) or full-spectrum scaled k-distribution (FSSK) method, depending on whether a correlated (FSCK) or a scaled (FSSK) absorption coefficient is assumed, respectively [13].

Similar to narrow band k-distributions these full-spectrum methods have LBL accuracy for homogeneous media, but at a tiny fraction of the computational cost. And, again, substantial inaccuracies can occur in nonhomogeneous media because the assumptions of a correlated or scaled absorption coefficient are violated, particularly in the presence of extreme temperature

* Corresponding author. Fax: +1-814-863-8682.
E-mail address: mfm6@psu.edu (M.F. Modest).
[1] Now with General Electric Corp., Schenectady, NY.

0017-9310/03/$ - see front matter © 2003 Elsevier Ltd. All rights reserved.
doi:10.1016/S0017-9310(03)00151-0

Nomenclature

a	weight function for FSCK method
A	parameter in the scaling function
b	self broadening-to-air-broadening coefficient
b_{self}	self-broadening line half-width, cm^{-1}
b_{air}	air-broadening line half-width, cm^{-1}
E	parameter in the scaling function, K
f	k-distribution function, cm
g	cumulative k-distribution
I	radiative intensity, $\text{W/m}^2\,\text{sr}$
k	absorption coefficient variable, cm^{-1}
k_η	spectral absorption coefficient at reference state, cm^{-1}
l	geometric length, m
n	scaling function parameter
p	pressure, bar
q	radiative heat flux, W/m^2
s, s'	distance along path, m
T	temperature, K
u	scaling function for absorption coefficient
w	quadrature weight
x	mole fraction

Greek symbols

η	wavenumber, cm^{-1}
$\underline{\phi}$	composition variable vector
Φ	scattering phase function
κ	absorption coefficient, cm^{-1}
Ω	solid angle, sr
σ_s	scattering coefficient, cm^{-1}

Subscripts

0	standard state for database
b	blackbody emission
j	line or bin
m	spectral group
max	maximum
min	minimum
P	Planck mean
ref	reference condition
w	wall
η	spectral

changes and/or changing mole fractions. To overcome this limitation, Pierrot et al. [10] developed the fictitious-gas-based absorption distribution function (ADFFG), in which the individual lines comprising the absorption coefficient were placed into separate groups based on their temperature dependence. While improving accuracy, the method becomes more expensive in cpu time by a factor of M^2, where M is the number of fictitious gases or groups. Similarly, Zhang and Modest [14] extended their FSK method to such fictitious gases. Their multi-scale full-spectrum k-distribution (MSFSK) method requires only M solutions to the radiative transfer equation (RTE), by treating line overlap in an approximate fashion.

Very recently, Modest and Zhang [12] developed a new multi-group method (MGFSK), in which spectral positions (with absorption coefficients consisting of contributions from many different lines) are placed into spectral groups according to their dependence on temperature and (partial) pressure (as opposed to the ADFFG and MSFSK methods, which place spectral lines into groups, each of them affecting the absorption coefficient over many different wavenumbers). Such a model avoids the problem of overlap between different groups, thus requiring only M RTE evaluations *without* need for further approximation. In addition, it allows the consideration of partial pressure dependence during the grouping process. A 32-group database for CO_2 was constructed as part of that paper and was tested using the new multi-group approach [12].

In this paper, a similar database for H_2O will be presented and tested with the MGFSK method. In addition, the databases for CO_2 and H_2O will be applied, together with the random overlap mixture approach, to a practical combustion problem. The HITEMP database [15] will be used in this paper to build up the database. As indicated by Modest and Bharadwaj [16], HITEMP displays some questionable behavior in the band wings of CO_2 at temperatures above 1500 K. However, the MGFSK model can be used with any other database. Total pressure variations could be incorporated as well, and will be considered in follow-up work.

2. Theoretical development

2.1. The MGFSK approach

For the convenience of the reader, a brief overview of MGFSK method by Zhang and Modest [12] will be given here. The starting point is the spectral RTE for an absorbing, emitting and scattering medium [17],

$$\frac{\mathrm{d}I_\eta}{\mathrm{d}s} = \kappa_\eta(\underline{\phi},\eta)[I_{\mathrm{b}\eta}(T) - I_\eta] - \sigma_s\left[I_\eta - \frac{1}{4\pi}\int_{4\pi} I_\eta(\hat{s}')\Phi(\hat{s},\hat{s}')\,\mathrm{d}\Omega'\right], \tag{1}$$

where $\underline{\phi}$ is a vector containing all the composition variables defining the state of the gas, i.e., $\underline{\phi} = (T, p, x)$,

where x is the mole fraction of the absorbing gas. Eq. (1) is subject to the restriction that scattering properties σ_s and Φ (as well as bounding wall reflectance) are gray. Spectral locations are then sorted into $M = 32$ spectral groups according to the absorption coefficient dependence on temperature and partial pressures. For the mth spectral group $[\eta_m]$ (containing all the wavenumbers for that group), the RTE is reordered as done for CO_2 [12] and one obtains

$$\frac{dI_{gm}}{ds} = k_m(T_{ref}, \underline{\phi}, g_m)[a_m(T, T_{ref}, g_m)I_b(T) - I_{gm}] - \sigma_s\left[I_{gm} - \frac{1}{4\pi}\int_{4\pi} I_{gm}(\hat{s}')\Phi(\hat{s}, \hat{s}')\,d\Omega'\right], \quad (2)$$

where

$$f_m(T, \underline{\phi}_{ref}, k_m) = \frac{1}{I_b(T)}\int_{\eta\in[\eta_m]} I_{b\eta}(T)\delta(k_m - \kappa_\eta(\underline{\phi}_{ref}, \eta))\,d\eta, \quad (3)$$

$$g_m(T_{ref}, \underline{\phi}_{ref}, k_m) = \int_0^{k_m} f_m(T_{ref}, \underline{\phi}_{ref}, k_m)\,dk_m, \quad (4)$$

$$I_{gm} = \int_{\eta\in[\eta_m]} I_\eta\delta(k_m - \kappa_\eta(\underline{\phi}_{ref}, \eta))\,d\eta / f_m(T_{ref}, \underline{\phi}_{ref}, k_m), \quad (5)$$

$$a_m(T, T_{ref}, g_m) = \frac{f_m(T, \underline{\phi}_{ref}, k_m)}{f_m(T_{ref}, \underline{\phi}_{ref}, k_m)}. \quad (6)$$

Here f_m is the Planck-function weighted k-distribution, determined based on the absorption coefficient evaluated at a reference state $\underline{\phi}_{ref}$, and g_m is its cumulative distribution, which acts as a nondimensional reordered wavenumber; I_{gm} is the resulting "spectral" intensity for group m, and a_m is a stretching factor for g_m between local temperature T and reference temperature T_{ref}. Note that the first argument of f_m is the Planck function temperature (i.e., temperature of the radiation source), while the second argument describes the state of the gas at which the absorption coefficient is evaluated (including the—usually different—gas temperature).

Evaluation of I_{gm} requires the precalculation of two sets of FSK for each of the M spectral groups: (i) k-distributions $f_m(T, \underline{\phi}_{ref}, k_m)$, evaluated for the absorption coefficient taken at reference conditions and for all Planck function temperatures (for the determination of a_m), and (ii) k-distributions $f_m(T_{ref}, \underline{\phi}, k_m)$, with the absorption coefficient evaluated at local conditions, but the Planck function only at the reference temperature [for the evaluation of $k(T_{ref}, \underline{\phi}, g_m)$]. Once I_{gm} has been found using any arbitrary RTE solution method, total intensity is determined by summing over all spectral groups and integrating over g-space, i.e.,

$$I = \int_0^\infty I_\eta\,d\eta = \sum_{m=1}^{M}\int_0^1 I_{gm}\,dg. \quad (7)$$

Note that the reference state $\underline{\phi}_{ref}$ is the only state where the absorption coefficient is taken in its exact form and that a correlated absorption coefficient is assumed for all other states. Therefore, it is important to choose an optimal reference state for each problem at hand. While any arbitrary value can be used for the reference Planck function temperature, it is usually set to the same value as the temperature of the reference state $\underline{\phi}_{ref}$. As stated, Eq. (2) uses a correlated absorption coefficient and, as such, should be termed the multi-group full-spectrum correlated k-distribution (MGFSCK) method; using a scaled absorption coefficient, on the other hand, would lead to the MGFSSK approach. For the fine nuances between a correlated and a scaled absorption coefficient the reader is referred to [13].

2.2. Databasing of spectral groups

Similar to the previous databasing of CO_2 [12], we start by observing the typical behavior of the absorption coefficient scaling function of water vapor

$$u_\eta(\underline{\phi}, \underline{\phi}_0, \eta) = \frac{\kappa_\eta(\underline{\phi}, \eta)}{\kappa_\eta(\underline{\phi}_0, \eta)}, \quad (8)$$

as it varies across the spectrum, where $\underline{\phi}_0$ is any arbitrary standard state to be compared with (and is not related to the reference state of the previous section). Some typical results are shown in Figs. 1 and 2 for a mixture containing 20% H_2O, for a few selected spectral locations across the 1500–1600 cm^{-1} (6.3 μm band) and 3900–4000 cm^{-1} (2.7 μm band) ranges. As for CO_2, this behavior was found to be consistent for all spectral locations, and also consistent with theoretical predictions

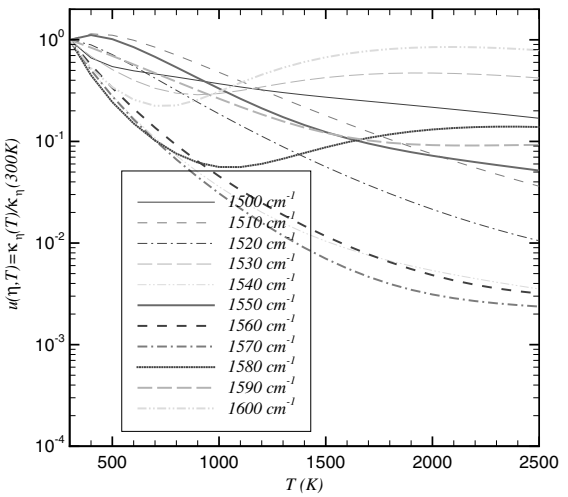

Fig. 1. Scaling function u_η for several spectral locations across the 1500–1600 cm^{-1} spectral range of H_2O, where $\underline{\phi}_0 = (300\ K, 1\ bar, 20\%)$.

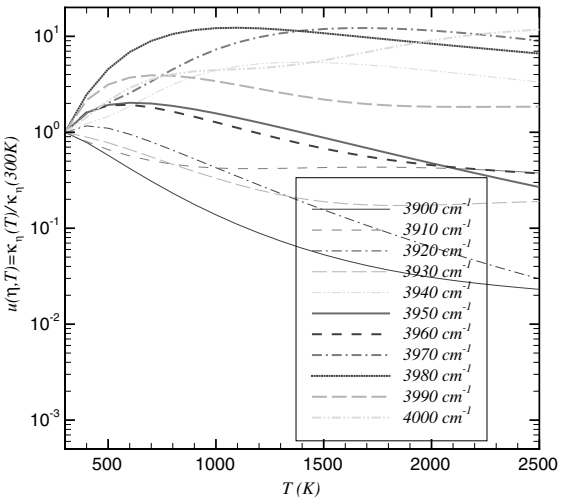

Fig. 2. Scaling function u_η for several spectral locations across the 3900–4000 cm^{-1} spectral range of H_2O, where $\underline{\phi}_0 = (300\ \text{K}, 1\ \text{bar}, 20\%)$.

of the absorption coefficient. Based on a thorough investigation of H_2O scaling function behavior, a set of 32 scaling functions was chosen as

$$u_m(T,x;T_0,x_0) = \frac{1+bx\sqrt{\frac{T_0}{T}}+A_m\left[1+bx\left(\frac{T_0}{T}\right)^2\right]e^{-E_m/T}}{1+bx_0\sqrt{\frac{T_0}{T}}+A_m\left[1+bx_0\left(\frac{T_0}{T}\right)^2\right]e^{-E_m/T_0}}\left(\frac{T_0}{T}\right)^{n_m}, \tag{9}$$

and are shown in Fig. 3 (here arbitrarily normalized with $T_0 = 300$ K and $x_0 = 0.2$ for better discernibility). In its parametric form, Eq. (9) is identical to the parametric

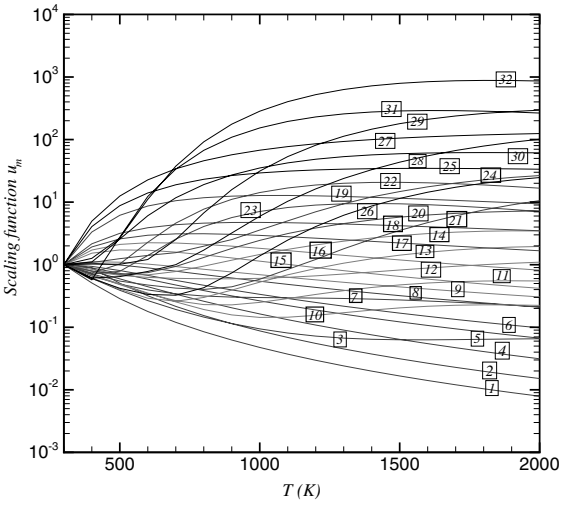

Fig. 3. Standard scaling functions u_m for H_2O.

form for CO_2, and can be expected to perform well for all gases. Each of the scaling functions is defined by the three parameters A_m, E_m and n_m, and a self broadening-to-air broadening coefficient defined as

$$b = \frac{b_{\text{self}}}{b_{\text{air}}} - 1, \tag{10}$$

where b_{self} is line width due to self broadening, and b_{air} the one due to air broadening. This ratio is fairly constant across the entire spectrum for all gases. For H_2O $b \simeq 4$, which was chosen for all 32 groups here. With the group of scaling functions defined, a scan is made across the entire spectrum (in steps of $\Delta\eta = 0.01$ cm^{-1}), evaluating the absorption coefficient from the HITEMP database [15] at a standard mole fraction of $x_0 = 0.2$, for a set of $J(=23)$ temperatures 300 K $\leqslant T_j \leqslant$ 2500 K. The spectral group into which wavenumber η_i is placed, $m(\eta_i)$, is found from minimization.

Once all wavenumbers of the spectrum have been placed into the 32 basic groups, FSK and the inverse of the cumulative k-distribution, $k_m(T_0, \underline{\phi}, g_m)$, can be calculated for each group and all states $\underline{\phi}$. If the absorption coefficient is correlated, then the ratio of two k-distributions for a given Planck function temperature, say T_0, but evaluated for absorption coefficients evaluated at different states $\underline{\phi}$ and $\underline{\phi}_0$, leads to a scaling function that depends on the cumulative k-distribution g_m [13]

$$u_{mg}(\underline{\phi}, \underline{\phi}_0, g_m) = \frac{k_m(T_0, \underline{\phi}, g_m)}{k_m(T_0, \underline{\phi}_0, g_m)}. \tag{11}$$

As an example, these scaling functions, for $\underline{\phi} = (2000\ \text{K}, 1\ \text{bar}, 20\%)$ and $\underline{\phi}_0 = (300\ \text{K}, 1\ \text{bar}, 20\%)$, are shown in Fig. 4 for all 32 spectral groups of H_2O. Note that, for each spectral group, the cumulative k-distribution ranges from a $g_{m,\min}$ to 1. A large range of $(1 - g_{m,\min})$ indicates that group m occupies a large part of the (Planck function weighted) spectrum. All ranges summed together must add to unity. Not surprisingly, the g-dependence of these scaling functions is weak: because of grouping criteria, the scaling function for each wavenumber comprising group m should have a scaling function closely following the standard function $u_m(\underline{\phi}, \underline{\phi}_0)$ of Eq. (9), i.e., should be independent of g_m. This is confirmed by Fig. 4; indeed, the g-dependence of the scaling functions for H_2O was found to be considerably weaker than for CO_2 indicating that, at the 32 group level, the absorption coefficient of H_2O is more scaled than that of CO_2. Therefore, at the 32-group level, we may assume the absorption coefficient not only to be correlated, but to be scaled, or

$$\kappa_\eta(\underline{\phi}, \eta) = \kappa_\eta(\underline{\phi}_0, \eta) u_m(\underline{\phi}, \underline{\phi}_0), \eta \in [\eta_m]. \tag{12}$$

This allows the construction of a much more compact database with little additional loss of accuracy. The standard state for the database is taken as $\underline{\phi}_0 =$

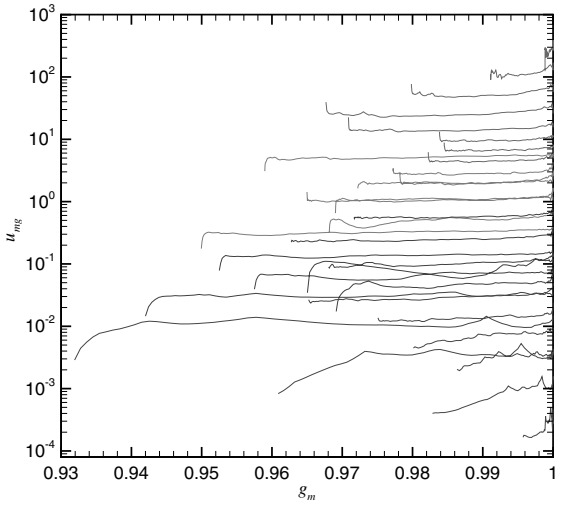

Fig. 4. Variation of actual scaling function u_{mg} (2000 K, 300 K, g_m) with cumulative k-distribution g_m for H_2O base groups.

($T_0 = 1500$ K, $p_0 = 1$ bar, $x_0 = 0.2$) simply for convenience, and should not be confused with the reference state ($\underline{\phi}_{\text{ref}}$) needed in Eq. (2) to recast the RTE as a function of cumulative k-distribution. Since the absorption coefficient is databased as scaled at the 32-group level, the choice of reference state for the 32GFSCK model is arbitrary. However, when groups are combined, the resulting absorption coefficient will no longer be scaled, and an optimal choice for the reference state becomes important.

With 32 groups for H_2O and the Planck function temperature ranging from 300 to 2500 K (23 temperatures), 32×23 k-distributions, $k_m(T, \underline{\phi}_0, g_m)$ ($m = 1, \ldots, 32$) have been evaluated and databased. The k-distributions at any nonstandard state $\underline{\phi}$ can then be calculated as

$$k_m(T, \underline{\phi}, g_m) = k_m(T, \underline{\phi}_0, g_m) u_m(\underline{\phi}, \underline{\phi}_0), \tag{13}$$

(with 32 values each for A_m, E_m and n_m also databased for the scaling functions u_m).

2.3. Weight function a

At this point, for each of the 32 spectral groups for H_2O the FSK have been calculated and databased. The required number of data points for each k-distribution and, thus, the efficiency of the database is greatly affected by the smoothness of the weight function a_m defined in Eq. (6). This function is the ratio of two k-distributions, or the ratio of the slopes of two cumulative k-distributions (evaluated at Planck function temperatures of T and T_{ref}, respectively). Therefore, the weight function is very sensitive to the structure of the k-distributions. Noisy weight functions will have detrimental effects on quadrature efficiency, in particular for groups with holes (ranges of absorption coefficient not present in the spectral group under consideration) in their k-distributions. Therefore, the k-distributions were smoothened, in order for them to produce smoothly varying weight functions a_m in the same way as was done for CO_2 [12]. Since different absorption coefficient regions may become important at different optical thicknesses, the database for the 32 groups of H_2O was constructed with 100 k-boxes (values) each, allowing the user to choose proper quadrature points, depending on the problem at hand. With 32 groups, 23 Planck function temperatures and 100 k-boxes (values) considered, the size of the resulting database is about 1 MB.

2.4. Combination of spectral groups

For greater numerical efficiency (accompanied by a slight loss of accuracy), the spectral groups from the database can be combined to obtain coarser group models ($N = 1, 2, 4, \ldots$). While the absorption coefficient may be assumed to be scaled at the 32 group level, this is clearly not true after combining groups, unless a new scaling function is determined after each grouping, following the guidelines of Modest and Zhang [11]. However, if we simply assume that each group has a correlated absorption coefficient, then, since there is no overlap between different spectral groups [12],

$$g_n(T, \underline{\phi}, k) = \sum_m g_m(T, \underline{\phi}, k) - N_n + 1, \quad n = 1, 2, \ldots, N \tag{14}$$

where n is the new group resulting from combining a number of basic groups and N_n is the number of base groups that have been combined to form group n. This relation may be inverted to give k_n as a function of the combined group's cumulative k-distribution g_n,

$$k_n(T, \underline{\phi}, g_n) = g_n^{-1}(T, \underline{\phi}, k_n). \tag{15}$$

This is demonstrated in Fig. 5, where Groups 3 and 4 were combined and the combined k-distribution essentially coincides with the k-distribution calculated directly from the HITEMP database (the only errors coming from the scaling in Eq. (13) and the smoothing of the databased k-distributions).

If all 32 groups are combined into one ($N = 1$) this results in FSK as required for the FSK models [11,13], evaluated accurately and efficiently from a small database (as opposed to tedious calculations from the HITEMP database).

2.5. Use of the database

Solving a general radiation problem using N different spectral groups requires the solution of the RTE, Eq. (2),

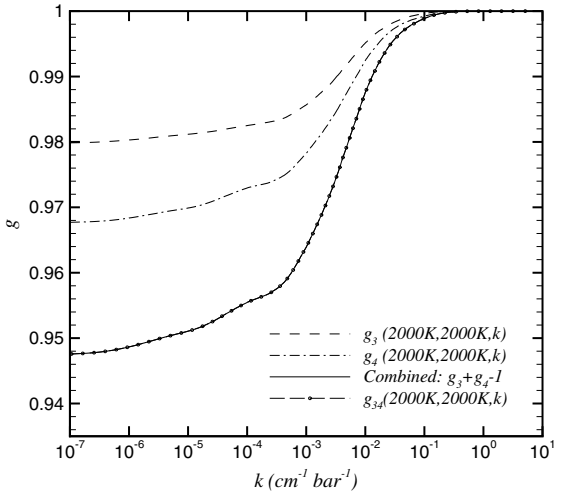

Fig. 5. Combination of two spectral groups into one (H_2O groups 3 and 4).

for each of these groups. This in turn, requires (i) definition of an optimal global reference state $\underline{\phi}_{\text{ref}}$, at which the absorption coefficient and its k-distribution are calculated "exactly"; (ii) precalculation of a set of k-distributions $k_n(T_{\text{ref}}, \underline{\phi}, g)$ for each group, i.e., absorption coefficient evaluated at local state $\underline{\phi}$, Planck function at T_{ref} (for use in Eq. (2)), and (iii) precalculation of a set of k-distributions $k_n(T, \underline{\phi}_{\text{ref}}, g)$ for each group, i.e., absorption coefficient evaluated at the reference state $\underline{\phi}_{\text{ref}}$, Planck function at local temperature T (for the evaluation of the weight function a_n). These distributions are extracted from the database, which contains for each of the $M = 32$ groups: (a) parameters A_m, E_m, n_m $(m = 1, M)$ for the evaluation of $u_m(\underline{\phi}, \underline{\phi}_0)$ from Eq. (9), and (b) k-distributions $k_m(T_j, \underline{\phi}_0, g)$ $(m = 1, M;\ j = 1, J)$ for $J = 23$ Planck function temperatures equally spaced between 300 and 2500 K.

Step 1: A global reference state is chosen along the guidelines of Modest and Zhang [11], i.e., the Planck mean temperature as reference temperature and the volume-averaged mole fraction as reference mole fraction.

Step 2: Keeping in mind that the database uses a standard state of $\underline{\phi}_0 = (T_0 = 1500\ \text{K},\ p_0 = 1\ \text{bar},\ x_0 = 20\%)$, one finds for each of the 32 groups

$$k_m(T, \underline{\phi}, g_m) = k_m(T, \underline{\phi}_0, g_m) u_m(\underline{\phi}, \underline{\phi}_0). \tag{16}$$

At this point $k_m(T, \underline{\phi}, g_m)$ is available for all Planck function temperatures (including T_{ref}) and local states $\underline{\phi}$ (including $\underline{\phi}_{\text{ref}}$) in the form of 23×100 pairs of points $(k_{m,i}, g_{m,i})$.

Step 3: If groups are to be combined into an N-group model for greater numerical efficiency, this is now done through the use of Eq. (14). In the database, groups are numbered in such a way that groups with similar scaling function u_m are always next to each other, so adjacent groups should be combined. This results in $N \times 100$ pairs of points $(k_{n,i}, g_{n,i})$ for the N combined groups.

Step 4: For all Planck function temperatures T, the weight functions $a_n(T, T_{\text{ref}}, g_n)$ are calculated from

$$a_{n,i} = \left.\frac{\mathrm{d}g_n(T, \underline{\phi}_{\text{ref}})}{\mathrm{d}g_n(T_{\text{ref}}, \underline{\phi}_{\text{ref}})}\right|_{k=k_{n,i}} \approx \frac{g_{n,i+1}(T, \underline{\phi}_{\text{ref}}) - g_{n,i-1}(T, \underline{\phi}_{\text{ref}})}{g_{n,i+1}(T_{\text{ref}}, \underline{\phi}_{\text{ref}}) - g_{n,i-1}(T_{\text{ref}}, \underline{\phi}_{\text{ref}})}. \tag{17}$$

(a_n is calculated indirectly from Eqs. (6) and (4) since only (smoothened) values of $g_n(k)$ are stored in the database).

Step 5: A set of J quadrature points, say $J = 10$, is chosen for the problem at hand to eventually carry out the integration in Eq. (7) as

$$I = \sum_{n=1}^{N} I_n = \sum_{n=1}^{N} \int_{g_{n,\min}}^{1} I_{g,n}\mathrm{d}g_n \approx \sum_{n=1}^{N} \sum_{j=1}^{J} w_j I_{g,n}(g_{n,j}), \tag{18}$$

where the w_j and $g_{n,j}$ are quadrature weights and points, respectively. For this operation, the data sets for $k_n(T_{\text{ref}}, \underline{\phi}, g_n)$ and $a_n(T, T_{\text{ref}}, g_n)$ are reduced to the corresponding J values each.

Step 6: Given the necessary set of k_n and a_n values, the RTEs for each of the n groups are solved and results collected according to Eq. (18).

3. Sample calculations

The new 32-group database for H_2O is tested in this section by calculating radiative heat loss rates from several one-dimensional slabs of gas mixtures with varying temperatures and mole fractions, using the multi-group approach [12]. A uniform mixture of 20% H_2O–80% N_2 (by volume) at 1 bar, confined between two infinite, parallel, cold and black plates, is considered first to test the validity of the model in situations of extreme temperature changes. In this problem, an isothermal layer at 2000 K with a fixed width of 50 cm is adjacent to another isothermal, cold layer at 300 K of varying width. The radiative heat flux exiting the cold column is shown in Fig. 6, with LBL calculations serving as benchmark. For simplicity, a simple trapezoidal rule was used in the LBL calculations (with a resolution of 0.01 cm^{-1}) and the accuracy of the LBL results are expected to be within ≈1%. The MGFSCK results calcu-

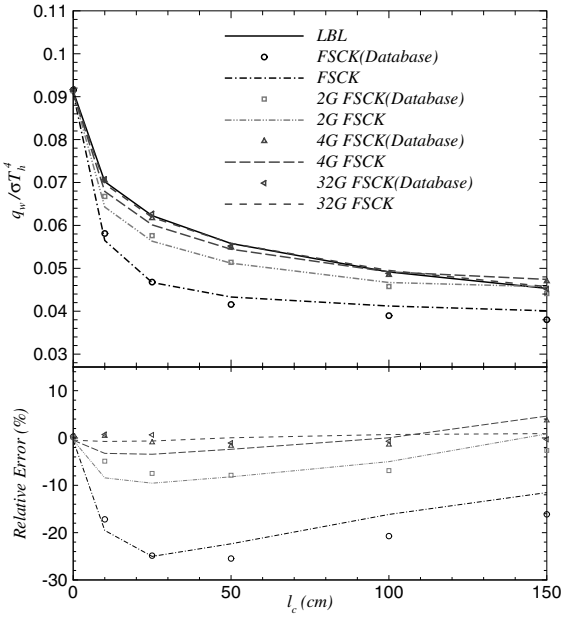

Fig. 6. Radiative flux exiting from the cold column of a two-column H_2O–nitrogen mixture at different temperatures (T_{hot} = 2000 K, l_{hot} = 50 cm; T_{cold} = 300 K, l_{cold} variable; uniform p = 1 bar, x_{H_2O} = 0.2, cold and black walls on both sides) and their relative error compared with the LBL benchmark.

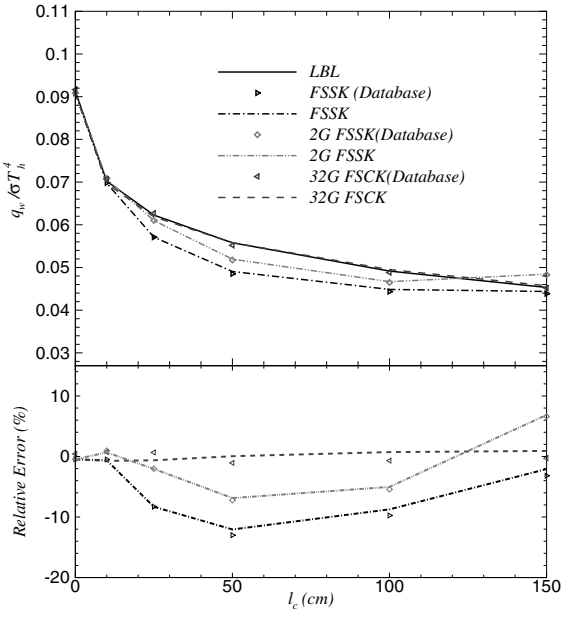

Fig. 7. Same as Fig. 6, but using multi-group FSSK model.

lated directly from the HITEMP database are shown by lines, while the symbols represent results using the 32-group database for H_2O. The 32-group model uses a scaled absorption coefficient and, is, thus, independent of the choice of reference state; for combined groups, the reference state recommended by Modest and Zhang [11] was used. As can be seen from Fig. 6, the direct FSCK results and those from the database are in very good agreement. Note that there is a substantial improvement when going from a single group model (FSCK) to a 2GFSCK model, with the maximum error changing from 25% to less than 9%. The improvement from 2GFSCK to 4GFSCK is not as large and LBL accuracy can essentially be achieved with eight or more groups (within the limits of quadrature error for both LBL and FSCK). Results using the k-distributions provided by the database (symbols) are very close to those using k-distributions obtained directly from the HITEMP database (lines); while some error accumulation is apparent, especially at the 1- and 2-group levels, the overall accuracy of the method remains unaffected by using the compact database.

Modest [13] has shown that using a scaled absorption coefficient is superior to the FSCK method if the scaling function is optimized, resulting in the FSSK method. This model can also be implemented with the 32 group database. The results for a single group FSSK and a 2GFSSK (results from both database and direct calculations from the HITEMP database) are shown in Fig. 7. The FSSK method considerably outperforms the FSCK result, reducing the maximum error from about 25% (FSCK) to 12% (FSSK), while 2GFSSK and 2GFSCK perform about equally well. Therefore, using the (in this case slightly more tedious) FSSK method makes sense only if all 32 groups are combined into a single group.

The same problem, but with a hot left wall at 1000 K, was also considered and the MGFSCK results are shown in Fig. 8. In this case, the single-group FSCK result has a maximum error of about 13%, which is improved to around 6% for 2GFSCK. With four or more groups the accuracy rivals that of LBL results.

The next example considers a H_2O–N_2 gas mixture with both a step in temperature and a step in mixture ratio. The medium is again a one-dimensional slab with a hot layer (2000 K, 10% H_2O, 50 cm width) adjacent to a cold layer (300 K, 50% H_2O, with varying cold layer width l_c). The wall next to the hot layer is at 1000 K and that next to the cold layer is at 0 K, with both walls black. The radiative heat flux exiting the cold column of this mixture is shown in Fig. 9, leading to the same conclusions as the results of Fig. 6. A number of other cases were studied and the same conclusions can be drawn: a substantial improvement occurs when going from a single group model to a 2GFSCK model; LBL accuracy is approached with a maximum of eight groups. However, combining groups using the assumption of a correlated absorption coefficient makes the

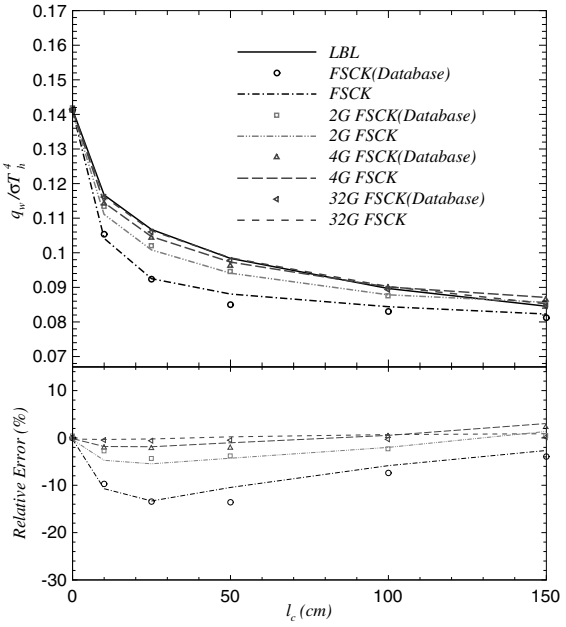

Fig. 8. Same as Fig. 6, except that the left wall is at 1000 K.

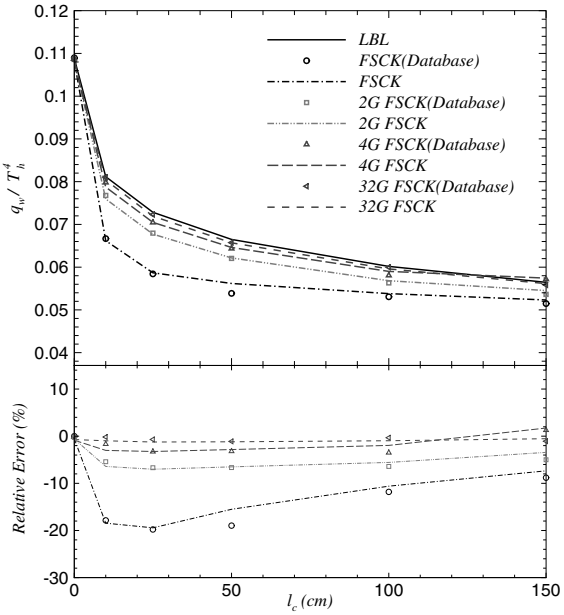

Fig. 9. Same as Fig. 6, except that $x_{\text{hot}} = 0.1$, $x_{\text{cold}} = 0.5$ and the left wall is at 1000 K.

8-group model dependent on the chosen reference state, $\underline{\phi}_{\text{ref}}$, and thus cannot be databased efficiently. For that reason, the database was collected for a 32-group model, which uses a *scaled* absorption coefficient and is, thus, independent of the reference state.

4. Incorporation of FSK model into CFD/combustion code

The FSK models have proven to be very successful in simplifying molecular gas radiation calculations from about 1 million (LBL) to only a few spectral calculations, thus making it possible to accurately predict the role of radiation in combustion systems. It will be shown in this section how the FSK model, as derived from the present database, can be interfaced with a CFD/combustion code (in this case, FLUENT [18]), to provide accurate predictions in a typical combustion environment, using the databases already built for CO_2 and H_2O. Since FLUENT's radiation solvers do not allow for truly nongray properties, the P_1-approximation was used, spectral renditions of which [17] are readily implemented in the form of FLUENT's 'additional scalar equations'.

4.1. Combustion test problem

An axisymmetric jet flame is considered and the geometry is shown in Fig. 10. A small nozzle in the center of the combustor introduces methane at 80 m/s, and ambient air enters the combustor coaxially at 0.5 m/s. The overall equivalence ratio is approximately 0.76 (about 28% excess air). The high-speed methane jet initially expands without interference from the outer wall, and entrains and mixes with the low-speed air. The Reynolds number based on the methane jet diameter is approximately 28,000. The combustion is modelled using a global, one-step reaction mechanism together with a finite-rate chemistry model. Since methane is consumed at relatively low temperature and is present only over a small fraction of the combustor volume, only the radiative effects of CO_2 and H_2O are considered. And because, for the single-group model to be employed here, the FSSK model is more accurate than the FSCK approach, it is used here together with the P_1-approximation to account for molecular gas radiation.

In principle, variable mixtures of different absorbing gases pose no additional difficulty, because the absorption coefficient of all species can simply be added up. In practice, however, it would be highly desirable to build k-distributions for arbitrary gas mixtures from k-distributions of individual species. For nonoverlapping absorption coefficients the cumulative k-distributions are additive as demonstrated earlier for the combination of

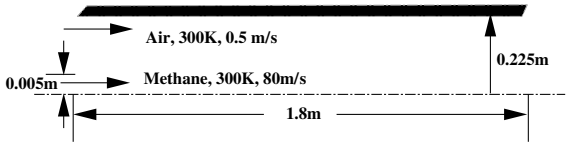

Fig. 10. Geometry of cylindrical combustor.

H_2O groups. On the other hand, if overlap is totally random the k-distributions can be considered as statistically uncorrelated, and one obtains from the multiplication approach [19,20] or random-overlap approach [17]

$$g(T,\underline{\phi},k) = g_{CO_2}(T,\underline{\phi},k) \times g_{H_2O}(T,\underline{\phi},k). \tag{19}$$

For CO_2–H_2O mixtures this approach has been rather successful on narrow band and full spectrum levels (i.e., for complete overlap of the spectral ranges for CO_2 and H_2O). Whether and how this approach can be applied to the multi-group model is unknown at this point, and will be the focus of a future study.

For the present test problem the new 32-group databases for CO_2 and H_2O are used, but all 32 groups are combined to obtain a set of single-group k-distributions each for CO_2 and H_2O, respectively. Eq. (19) is then used to obtain the k-distributions for the mixture.

The problem is first solved using a finite volume code (FLUENT) without considering radiation effects. Since fuel is injected from the inlet together with cold air, temperatures near the inlet are relatively low (≈300 K). The combustion reaction produces a flame sheet with high downstream outlet temperatures. Temperature levels inside the chamber range from 300 K to around 2400 K, as shown in Fig. 11(a). The single-group FSSK model was then incorporated into FLUENT to account for radiation. A reference state (Planck mean reference temperature and a volume averaged mole fraction) was first chosen, based on the temperature and mole fraction distributions obtained above (without radiation). The database is then converted and combined into single groups for each specie using Eq. (14). Assuming that the spectral overlap between CO_2 and H_2O is random, Eq. (19) is used to calculate the k-distributions for the gas mixture. The scaling function u is calculated at this point for all gas temperatures and partial pressures. Following the choice of 10 quadrature points (10 k (or g) values and 10 weights), the weight function a is calculated for all Planck function temperatures at those 10 quadrature values.

All precalculations (the 10 k values, 10 quadrature weights, weight functions a and scaling functions u) were input into FLUENT and 10 user defined scalars (see FLUENT manual [18]) were defined and solved using FLUENT solvers. During each iteration, the radiative heat source and radiative heat flux were determined and coupled into the energy equation. The converged temperature field is shown in Fig. 11(b). As is well known, radiation makes the flame colder on average, with the peak temperature dropping to 2150 K. The mole fraction distributions for CO_2 and H_2O are shown in Fig. 12 for the FSSK model. Due to the use of a single global reaction for methane the mole fraction of H_2O is everywhere twice that of CO_2.

To ensure that the FSSK model accurately predicts the radiation field for the present problem, the temperature field shown in Fig. 11(b) and the mole fraction fields shown in Fig. 12 were also used to make a LBL calculation. The radiative heat source $\nabla \cdot \mathbf{q}$ determined from LBL calculations for this case is shown in Fig. 13(a) and the relative error of the FSSK model with respect to the LBL benchmark, defined as

$$\text{error } (\%) = \frac{\nabla \cdot \mathbf{q}_{LBL} - \nabla \cdot \mathbf{q}_{FSSK}}{|\nabla \cdot \mathbf{q}_{LBL}|_{max}} \times 100 \tag{20}$$

is shown in Fig. 13(b). It can be seen that the maximum errors are about 4%. Thus, one may conclude that the FSSK model, in general, predicts heat transfer rates very well, and that the 32-group databases allow efficient and accurate implementation of the FSSK model. In this case, the radiation loss from the flame reduces the maximum temperature by as much as 250 K.

Combustion gases are sometimes treated as gray in order to simplify calculations. For comparison, a gray

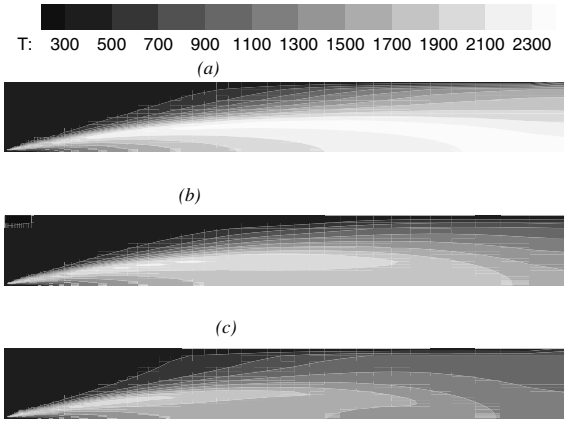

Fig. 11. Jet flame temperature contours: (a) without considering radiation, (b) considering radiation using the FSSK model, (c) considering gray radiation.

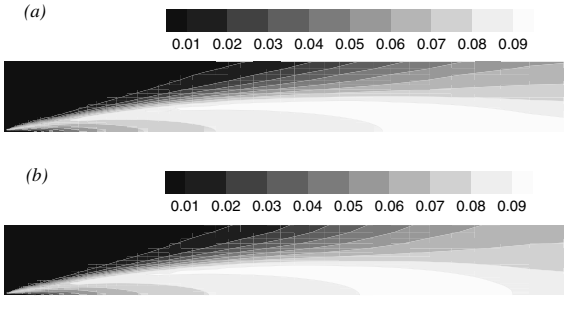

Fig. 12. Mole fraction distribution in a two-dimensional cylindrical combustion chamber for CO_2 and H_2O: (a) $x_{CO_2} = 0.5x_{H_2O}$ without radiation, (b) $x_{CO_2} = 0.5x_{H_2O}$ FSSK model.

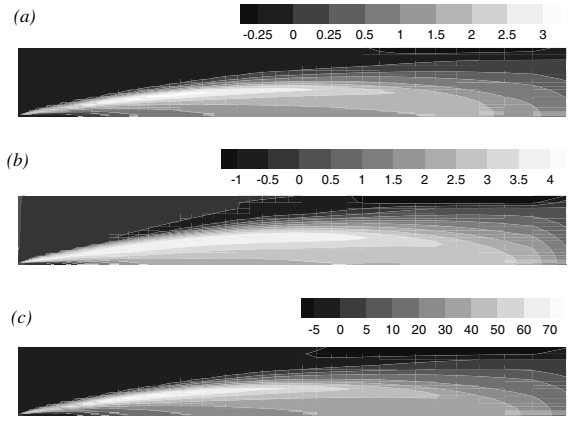

Fig. 13. 2D cylindrical combustion chamber with a gas mixture containing CO_2 and H_2O: (a) LBL calculations for the radiative heat source $\nabla \cdot \mathbf{q}$ (W/cm^3), (b) relative error of FSSK results, $(\nabla \cdot \mathbf{q}_{\mathrm{LBL}} - \nabla \cdot \mathbf{q}_{\mathrm{FSCK}})/\nabla \cdot \mathbf{q}_{\mathrm{LBL,max}}$, (c) relative error of gray radiation results.

radiation model was also implemented for the present combustor, with the local Planck mean absorption coefficient taken as the gray locally varying absorption coefficient. From the temperature contours shown in Fig. 11(c), one can see that the gray model strongly overpredicts radiative heat losses by as much as 80% (with the peak temperature dropping to 2050 K). The error of the radiative heat source based on the gray radiation model is shown in Fig. 13(c), indicating that treating gases as gray may cause large errors and is generally unacceptable in combustion applications, especially for optically thick flames.

5. Summary and conclusions

A 32-group database based on HITEMP was constructed for H_2O for use with the MGFSCK model, in which spectral locations are broken up into $N = 1, 2, 4, \ldots$ spectral groups, based on their absorption coefficient dependence on (partial) pressure and temperature. The database can also be employed for accurate and efficient evaluation of FSK for use in global radiation models, such as the FSSK, FSCK, SLW and ADF methods. The database was tested for problems with large temperature gradients and sharp concentration changes. A practical combustion problem was also considered to test the accuracy of the databases for CO_2 and H_2O mixtures. It was found that the MGFSCK model and the H_2O database provide very accurate results for radiative heat transfer calculations, approaching LBL accuracy at a very affordable cost. The database for H_2O has a size of less than 1 MB and is available upon request. Present limitations of the MGFSCK model are the lack of a mixing model at the multi-group level for CO_2–H_2O mixtures and, as for all global models, further investigation is required to address nongray boundaries and/or nongray scattering.

Acknowledgement

The authors gratefully acknowledge the financial support of the National Science Foundation under the contract CTS-0112423.

References

[1] A.A. Lacis, V. Oinas, A description of the correlated k-distribution method for modeling nongray gaseous absorption, thermal emission, and multiple scattering in vertically inhomogeneous atmospheres, J. Geophys. Res. 96 (D5) (1991) 9027–9063.
[2] R.M. Goody, Y.L. Yung, Atmospheric Radiation—Theoretical Basis, second ed., Oxford University Press, New York, 1989.
[3] R.M. Goody, R. West, L. Chen, D. Crisp, The correlated k-method for radiation calculations in non-homogeneous atmospheres, J. Quant. Spectrosc. Radiat. Transfer 42 (1989) 539–550.
[4] Q. Fu, K.N. Liou, On the correlated k-distribution method for radiative transfer in nonhomogeneous atmospheres, J. Atmos. Sci. 49 (22) (1992) 2139–2156.
[5] M.K. Denison, B.W. Webb, A spectral line based weighted-sum-of-gray-gases model for arbitrary RTE solvers, J. Heat Transfer 115 (1993) 1004–1012.
[6] M.K. Denison, B.W. Webb, The spectral-line-based weighted-sum-of-gray-gases model in nonisothermal nonhomogeneous media, J. Heat Transfer 117 (1995) 359–365.
[7] H.C. Hottel, A.F. Sarofim, Radiative Transfer, McGraw-Hill, New York, 1967.
[8] M.F. Modest, The weighted-sum-of-gray-gases model for arbitrary solution methods in radiative transfer, J. Heat Transfer 113 (3) (1991) 650–656.
[9] Ph. Rivière, A. Soufiani, M.Y. Perrin, H. Riad, A. Gleizes, Air mixture radiative property modelling in the temperature range 10,000–40,000 K, J. Quant. Spectrosc. Radiat. Transfer 56 (1996) 29–45.
[10] L. Pierrot, Ph. Rivière, A. Soufiani, J. Taine, A fictitious-gas-based absorption distribution function global model for radiative transfer in hot gases, J. Quant. Spectrosc. Radiat. Transfer 62 (1999) 609–624.
[11] M.F. Modest, H. Zhang, The full-spectrum correlated k-distribution for thermal radiation from molecular gas–particulate mixtures, J. Heat Transfer 124 (1) (2002) 30–38.
[12] H. Zhang, M.F. Modest, Scalable Multi-group full-spectrum correlated k-distributions for radiative heat transfer, J. Heat Transfer 125 (3) (2003).
[13] M.F. Modest, Narrow-band and full-spectrum k-distributions for radiative heat transfer—correlated-k vs. scaling approximation, J. Quant. Spectrosc. Radiat. Transfer 76 (1) (2003) 69–83.
[14] H. Zhang, M.F. Modest, A multi-scale full-spectrum correlated k-distribution for radiative heat transfer in

inhomogeneous gas mixtures, J. Quant. Spectrosc. Radiat. Transfer 73 (2–5) (2002) 349–360.

[15] L.S. Rothman, C. Camy-Peyret, J.-M. Flaud, R.R. Gamache, A. Goldman, D. Goorvitch, R.L. Hawkins, J. Schroeder, J.E.A. Selby, R.B. Wattson, HITEMP, the High-Temperature Molecular Spectroscopic Database, 2000, available through http://www.hitran.com.

[16] M.F. Modest, S.P. Bharadwaj, High-resolution high-temperature transmissivity measurements and correlations for carbon dioxide–nitrogen mixtures, J. Quant. Spectrosc. Radiat. Transfer 73 (2–5) (2002) 329–338.

[17] M.F. Modest, Radiative Heat Transfer, second ed., Academic Press, New York, 2003.

[18] Fluent, FLUENT 6.0 UDF Manual, Fluent Inc., New Hampshire, 2001.

[19] M.K. Denison, B.W. Webb, The spectral-line weighted-sum-of-gray-gases model for H_2O/CO_2 mixtures, J. Heat Transfer 117 (1995) 788–792.

[20] V. Solovjov, B.W. Webb, SLW modeling of radiative transfer in multicomponent gas mixtures, J. Quant. Spectrosc. Radiat. Transfer 65 (2000) 655–672.